



저작자표시-비영리-변경금지 2.0 대한민국

이용자는 아래의 조건을 따르는 경우에 한하여 자유롭게

- 이 저작물을 복제, 배포, 전송, 전시, 공연 및 방송할 수 있습니다.

다음과 같은 조건을 따라야 합니다:



저작자표시. 귀하는 원저작자를 표시하여야 합니다.



비영리. 귀하는 이 저작물을 영리 목적으로 이용할 수 없습니다.



변경금지. 귀하는 이 저작물을 개작, 변형 또는 가공할 수 없습니다.

- 귀하는, 이 저작물의 재이용이나 배포의 경우, 이 저작물에 적용된 이용허락조건을 명확하게 나타내어야 합니다.
- 저작권자로부터 별도의 허가를 받으면 이러한 조건들은 적용되지 않습니다.

저작권법에 따른 이용자의 권리는 위의 내용에 의하여 영향을 받지 않습니다.

이것은 [이용허락규약\(Legal Code\)](#)을 이해하기 쉽게 요약한 것입니다.

[Disclaimer](#)

Discovery of new gene of therapeutics to suppress drug resistance of pancreatic cancer

Myeong Jin Kim

Department of Medical Science

The Graduate School, Yonsei University

Discovery of new gene of therapeutics to suppress drug resistance of pancreatic cancer

Directed by Professor Jae-Ho Cheong

The Master's Thesis
submitted to the Department of Medical Science,
the Graduate School of Yonsei University
in partial fulfillment of the requirements for the degree of
Master of Medical Science

Myeong Jin Kim

December 2023

This certifies that the Master's Thesis
of Myeong Jin Kim is approved.

Thesis Supervisor : Jae-Ho Cheong

Thesis Committee Member#1 : Joon Seong Park

Thesis Committee Member#2 : SungSoon Fang

The Graduate School
Yonsei University

December 2023

<TABLE OF CONTENTS>

ABSTRACT	IV
I. INTRODUCTION	1
II. MATERIALS AND METHODS	4
1. The Cancer Genome Atlas analysis	4
2. Cell culture	4
3. Patient's tissues mRNA and protein	4
4. Small-Interfering RNA transfection	5
5. WST assay	5
6. Wound healing	5
7. Invasion assay	5
8. RNA sequencing	6
9. Glutamine uptake assay	6
10. OCR and ECAR measurement	6
11. Glutathione level assay	7
12. ROS and lipid ROS measurement	7
13. RT-PCR and qPCR	7
14. Western blotting	8
15. Animal studies	8
16. Statistical	9
III. RESULTS	10
1. Expression of SLC38A5 in pancreatic cancer	10
2. SLC38A5 correlates with gemcitabine-resistance in pancreatic cancer	13
3. Deletion of SLC38A5 down-regulates cell viability and migration in	

gemcitabine-resistance pancreatic cancer cells.	17
4. Inhibition of SLC38A5 induces changes in ferroptosis-regulating genes	21
5. SLC38A5 regulates glutathione synthesis and related genes	25
6. SLC38A5 modulates lipid ROS through GSH-mediated ROS and mTOR-SREBP1 signaling in gemcitabine-resistance pancreatic cancer cells	29
7. Inhibition of SLC38A5 induces ferroptosis in gemcitabine-resistance pancreatic cancer cells.	34
8. Knockdown of SLC38A5 suppress tumor growth and metastasis in vivo	38
IV. DISCUSSION	43
V. CONCLUSION	45
REFERENCES	46
ABSTRACT(IN KOREAN)	50

LIST OF FIGURES

Figure 1. Expression of SLC38A5 in pancreatic cancer	11
Figure 2. SLC38A5 correlates with gemcitabine-resistance in pancreatic cancer	14
Figure 3. Deletion of SLC38A5 down-regulates cell viability and migration in gemcitabine-resistance pancreatic cancer cells	18
Figure 4. Inhibition of SLC38A5 induces changes in ferroptosis-regulating genes.....	22
Figure 5. SLC38A5 regulates glutathione synthesis and related genes	26
Figure 6. SLC38A5 modulates lipid ROS through GSH-mediated ROS and mTOR-SREBP1 signaling in gemcitabine-resistance pancreatic cancer cells	31
Figure 7. Inhibition of SLC38A5 induces ferroptosis in gemcitabine-resistance pancreatic cancer cells	35
Figure 8. Knockdown of SLC38A5 suppress tumor growth and metastasis in vivo	39
Figure 9. The graphical abstract illustrates the regulatory mechanism of SLC38A5 in gemcitabine-resistance pancreatic cancer	42

ABSTRACT

Discovery of new gene of therapeutics to suppress drug resistance of pancreatic cancer

Myeong Jin Kim

*Department of Medical Science
The Graduate School, Yonsei University*

(Directed by Professor Jae-Ho Cheong)

Pancreatic cancer has a poor prognosis with its five-year survival rate lower than that of any other cancer type because it is difficult to detect in the early stages. Gemcitabine, a standard treatment for pancreatic cancer, often has poor outcomes for patients as a result of chemoresistance. Therefore, novel therapeutic targets must be identified to overcome gemcitabine-resistance. Here, I found that SLC38A5, a glutamine transporter, is more highly overexpressed in gemcitabine-resistant patients than in gemcitabine-sensitive patients. Furthermore, the deletion of SLC38A5 decreased the proliferation and migration of gemcitabine-resistant PDAC cells. I also found that the inhibition of SLC38A5 triggered the ferroptosis signaling pathway via RNA sequencing. Also, silencing SLC38A5 induced mitochondrial dysfunction and reduced glutamine uptake and glutathione (GSH) levels, and downregulated the expressions of GSH-related genes NRF2 and GPX4. The blockade of glutamine uptake negatively modulated the mTOR-SREBP1-SCD1 signaling pathway. Therefore, suppression of SLC38A5 triggers ferroptosis via two pathways that regulate lipid ROS levels.

Similarly, I observed knockdown of SLC38A5 restored gemcitabine sensitivity by hindering tumor growth and metastasis in the orthotopic mouse model. Altogether, my results demonstrated that SLC38A5 could be a novel therapeutic target to overcome gemcitabine-resistance in PDAC therapy.

Key words: SLC38A5, gemcitabine-resistance, PDAC, lipid ROS, ferroptosis

Discovery of new gene of therapeutics to suppress drug resistance of pancreatic cancer

Myeong Jin Kim

*Department of Medical Science
The Graduate School, Yonsei University*

(Directed by Professor Jae-Ho Cheong)

I. INTRODUCTION

Pancreatic cancer is a lethal and aggressive cancer having less than 10% of a five-year survival rate¹. Because it is difficult to detect early, most patients have pancreatic cancer at an advanced stage, which lowers the success rate of surgical treatment. Therefore, these patients tend to receive chemotherapy^{2,3}. Currently, gemcitabine is one of the most widely used medications for the treatment of patients with pancreatic cancer⁴. However, the effects of gemcitabine are limited because drug resistance occurs within weeks of treatment⁵. Therefore, gemcitabine-resistance must be controlled as a key factor causing poor prognosis. Because there are only a few studies on gemcitabine-resistance in pancreatic cancer, a new strategy is necessary to alleviate drug resistance in pancreatic cancer.

Solute carrier family 38 membrane 5 (SLC38A5), also known as sodium-coupled neutral amino acid transporter 5 (SNAT5), transports amino acids such as asparagine, glutamine, methionine, serine, and glycine across the cell membrane⁶. Unlike other amino acid transporters, SLC38A5 mainly transports

glutamine into the cancer cells^{7,8}. For example, upregulation of SLC38A5 induces cell proliferation by inducing macropinocytosis in triple-negative breast cancer⁹. Moreover, a previous study reported that SLC38A5 initiates pancreatic neuroendocrine tumor formation¹⁰. However, there have been no studies on the biological mechanisms of SLC38A5 and gemcitabine-resistance in pancreatic cancer. This needs to be clarified in this study. According to The Cancer Genome Atlas (TCGA) database, upregulation of SLC38A5 tends to result in a poor survival rate in pancreatic cancer. Therefore, in this study, I hypothesized that there could be a crucial role of SLC38A5 in pancreatic cancer.

Glutamine is an important nutrient in cancer metabolism and is involved in the synthesis of proteins and lipids and de novo glutathione production¹¹. Cancer cells tend to consume more glutamine than normal cells during cell proliferation and epithelial-to-mesenchymal transition (EMT)¹². However, the correlation between glutamine and gemcitabine-resistance in pancreatic cancer remains unclear. Therefore, I aimed to study the effect of glutamine transported on SLC38A5 on gemcitabine-resistance. As glutamine enters cells, it is converted into glutamate via glutaminolysis in the mitochondria¹³. Eventually, glutamate is secreted from the mitochondria and contributes to glutathione synthesis¹⁴. Glutathione is an antioxidant that regulates reactive oxygen species (ROS) levels in cancer cells¹⁵. Additionally, glutamine regulates the mTOR-SREBP1 signaling pathway in cancer cells¹⁶. SCD1 is a downstream target gene of SREBP1 signaling and plays a role in converting Polyunsaturated fatty acids (PUFAs) that induce lipid ROS into monounsaturated fatty acids (MUFAs)¹⁷. Therefore, glutamine deprivation upregulates lipid ROS levels in pancreatic cancer cells. Hence, I hypothesized that glutamine depletion may increase the effect of gemcitabine on

gemcitabine-resistant pancreatic cancer cells.

Ferroptosis is a type of programmed cell death associated with lipid ROS accumulation¹⁸. Recently, several studies have shown that ferroptosis plays an important role in various cancers, including pancreatic cancer. Previous studies have shown that ferroptosis alleviates sorafenib resistance in hepatocellular carcinoma and cisplatin resistance in head and neck cancers^{19,20}. However, the relationship between ferroptosis and gemcitabine-resistance in pancreatic cancer has not been studied. Therefore, understanding these phenomena is important. In this study, I examined ROS and lipid ROS-related genes as indicators of ferroptosis²¹.

In this study, I observed that glutamine uptake was increased in gemcitabine-resistant pancreatic cancer. Moreover, the upregulated glutamine levels ultimately contribute to the inhibition of ferroptosis, making pancreatic cancer more resistant to gemcitabine. Conversely, gemcitabine-resistance was weakened when SLC38A5 expression was suppressed. I also confirmed that the depletion of SLC38A5 induces mitochondrial dysfunction and ROS levels and decreases mTOR-SREBP1 signaling. These pathways ultimately induce ferroptosis by increasing lipid ROS levels. Moreover, SLC38A5 inhibition effectively sensitizes pancreatic cancer cells to gemcitabine treatment, thereby suppressing tumor weight and metastasis *in vivo*. Taken together, my results suggest that SLC38A5 is a novel therapeutic target for ameliorating gemcitabine-resistance in pancreatic cancer.

II. MATERIALS AND METHODS

1. The Cancer Genome Atlas analysis

Expression data for pancreatic cancer were obtained from TCGA, and SLC38A5 levels were analyzed with transcripts per million (TPM) as $\log_2(\text{TPM} + 1)$ in the Gene Expression Profiling Interactive Analysis (GEPIA) portal. Clinical parameters and survival data were also acquired from TCGA pancreatic cancer database. Overall survival and disease-specific survival were analyzed using Kaplan-Meier plots. Correlation analysis of indicated genes was evaluated in GEPIA portal.

2. Cell culture

Human pancreatic cancer cell lines (PANC-1 and Capan-1) were purchased from American Type Culture Collection (ATCC MD, VA, USA). PANC-1 and Capan-1 were cultured in DMEM and RPMI 1640 supplemented with 10% fetal bovine serum (Biowest, Nuaille, France), and 1% antibiotic-antimycotic reagent (Gibco, Waltham, MA, USA) at 37°C and 5% CO₂. After one passage, gemcitabine was treated to PANC-1 and Capan-1 cells to establish gemcitabine-resistant cell line. After that, the surviving cells were subcultured and continuously treated with increasing gemcitabine concentration (0.1 uM to 10 uM) for 3 months. After the gemcitabine-resistant cells stabilized, they were treated with the same concentration of gemcitabine for 3 months.

3. Patient's tissues mRNA and protein

Pancreatic tissues were obtained from patients diagnosed with pancreatic cancer at Gangnam Severance Hospital. mRNA samples were isolated using the TRIZOL reagent (Sigma-Aldrich, Munich, Germany). Protein samples were extracted using RIPA lysis buffer (Sigma-Aldrich). The study protocol conformed to the ethical guidelines of the Declaration of Helsinki and was approved by the Institutional Review Board (IRB) of Gangnam Severance Hospital (no.3-2021-0414).

4. Small-Interfering RNA transfection

The cells were transfected with small-interfering RNA (siRNA) targeting SLC38A5 (Santa Cruz Biotechnology, Dallas, TX, USA) using Lipofectamine[®] RNAiMAX transfection reagent (Invitrogen, Waltham, Massachusetts, USA) in Opti-MEM (GIBCO) according to the manufacturer's protocol.

5. WST assay

The cells were seeded in 96-well plates at a density of 5×10^3 (PANC-1) and 7×10^3 (Capan-1) cells per well and incubated for 24 h. They were then treated with the indicated concentrations of gemcitabine for 72 h. Growth medium was replaced with 10% water-soluble tetrazolium (WST)-1 reagent (DoGenBio) and incubated for 1 h at 37°C in the dark. The absorbance of each well was measured at 450 nm wavelength using a VersaMax microplate reader (Molecular Devices, San Jose, CA, USA).

6. Wound healing assay

The cells were seeded in 12-well plates at densities of 2×10^5 (PANC-1) and 4×10^5 (Capan-1) per well. The next day, they were transfected with siRNA, and wound scratches were made 24 h after transfection. Microscopic images of the migrated cells were captured at the indicated time intervals.

7. Invasion assay

For invasion assay, 8- μ m pore size Transwell system was coated with Matrigel for 1 h at room temperature. The cells were seeded in 24-well plates at a density of 1×10^5 (PANC-1) and 2×10^5 (Capan-1). Cells were then transfected with siRNA. After 24h, cells were transferred to the transwell at a density of 0.7×10^5 (PANC-1) and 2.5×10^5 (Capan-1) and incubated for 24 h. The transwell plate was washed with PBS and fixed in 4% paraformaldehyde for 5 min. The transferred cells were stained with crystal

violet (JUNSEI, Tokyo, Japan).

8. RNA sequencing

Total RNA was isolated using the TRIzol reagent (Invitrogen). RNA quality was assessed using an Agilent 2100 Bioanalyzer with an RNA 6000 Nano Chip (Agilent Technologies, Amstelveen, The Netherlands), and RNA quantification was performed using an ND-2000 Spectrophotometer (Thermo Inc., DE, USA). For control and test RNAs, library construction was performed using QuantSeq 3' mRNA-Seq Library Prep Kit (Lexogen, Inc., Austria), according to the manufacturer's instructions. High-throughput sequencing was performed as 75-bp single-end sequencing using NextSeq 500 (Illumina, Inc., USA). QuantSeq 3 mRNA-Seq reads were aligned using the Bowtie2 (Langmead and Salzberg, 2012).

9. Glutamine uptake assay

The cells were seeded in a 6-well plate at a density of 2.5×10^5 (PANC-1) and 5×10^5 (Capan-1) per well. The next day, they were transfected with siRNA and harvested using lysis buffer and prepared for the measurement of glutamine using the Glutamine Detection Assay Kit (ab197011) from Abcam (Cambridge, U.K.), according to the manufacturer's instructions. Relative glutamine uptake was normalized to the number of cells in each experimental group.

10. OCR and ECAR measurement

The Oxygen consumption rate (OCR) was measured using a Seahorse XF24 extracellular flux analyzer (Seahorse Bioscience, North Billerica, MA, USA). The cells were seeded onto XF-24 plates at a density of 5×10^5 cells/well for 24 h and treated with siRNA. Thereafter, they were incubated XF assay media for 1 h at 37°C in a non-CO₂ incubator and stressed with sequential addition of 1 μM oligomycin, 2 μM carbonyl cyanide p-(trifluoromethoxy) phenylhydrazone, and a 0.5 μM cocktail of

rotenone/antimycin A. The OCR was normalized to the total cellular protein concentration.

11. Glutathione level assay

The cells were seeded in a 6-well plate at a density of 2.5×10^5 (PANC-1) and 5×10^5 (Capan-1) per well. The next day, they were transfected with siRNA and collected by scraping and prepared for the measurement of glutathione using the Glutathione Assay Kit (No. 703002) from Cayman Chemical (Michigan, USA) according to the manufacturer's protocol. Glutathione concentrations were calculated using a standard curve and normalized to the total protein levels in each sample.

12. ROS and lipid ROS measurement

The cells were seeded in a 6-well plate at a density of 2.5×10^5 (PANC-1) and 5×10^5 (Capan-1) per well. The next day, they were transfected with siRNA and treated with fer-1 (20uM) for 48 h. After treatment, they were incubated with 20 μ M 2',7'-dichlorodihydrofluorescein diacetate (DCF-DA; Sigma-Aldrich) and 10uM BODIPY-C11 (D3861, Invitrogen) for 30 min at 37°C in the dark. They were then washed twice with PBS. The ROS and lipid ROS levels were measured by fluorescence using a FACScanto II flow cytometer (BD Biosciences). A minimum of 10,000 events was recorded for each sample.

13. RT-PCR and qPCR

The cells were seeded in a 6-well-plate and incubated for 24 h, and then transfected with siRNA. RNA was isolated using the TRIZOL reagent. The isolated total RNA samples were analyzed by RT-PCR using a Maxime RT-PCR premix kit (Intron, Gyeonggi-do, Korea). RT-qPCR was performed using SYBR qPCR reaction mix (Applied Biosystems, Foster City, CA, USA). The primer sequences used in this study are listed in table 1. Relative mRNA expression level was calculated using the

2- $\Delta\Delta$ CT method, with GAPDH as the reference gene.

14. Western blotting

Cell lysates were separated using sodium dodecyl sulfate-polyacrylamide gel electrophoresis and transferred to polyvinylidene fluoride membranes. After blocking with 5% skim milk for 1 h, the membranes were incubated with primary antibodies (1:1000) at 4 °C overnight, followed by incubation with horseradish peroxidase (HRP)-conjugated secondary antibodies (1:5000) for 1 h. The protein bands were then exposed to an enhanced chemiluminescent HRP substrate (Waltham, MA, USA) and detected using X-ray film. The primary antibodies: GAPDH (# sc-365062), NRF2 (# sc-365949), GPX4 (# sc-166570), SREBP1 (# sc-17755) SCD1 (# sc-515844) were purchased from Santa Cruz Biotechnology (Dallas, TX, USA). mTOR (# 2972S), Phospho-mTOR (# 5536S), PI3K (# 4292S), pAKT (# 9271S), AKT (# 9272S), pSTAT3 (# 9145S), STAT3 (# 9139S) were purchased from Cell Signaling Technology (Danvers, MA, USA). SLC38A5 (# ab72717), RRM1 (# ab226391) were purchased from Abcam. N-cadherin (# 610920) and E-cadherin (# 610181) antibodies were purchased from BD Biosciences (Franklin Lakes, New Jersey, USA). Horseradish peroxidase-conjugated goat anti-mouse (# 7076S) and HRP-conjugated goat anti-rabbit (#7074S) secondary antibodies were purchased from Cell Signaling Technology.

15. Animal studies

Six-week-old male nude BALB/c mice were purchased from Orient Bio (Tokyo, Japan). To establish the orthotopic mouse model, 3×10^6 PANC-1 cells were injected into the pancreas of each mouse. After two months, the mice were randomized into two sensitive groups (n = 6) and three resistance groups (n = 6). Then, 4.5×10^6 shRNA lentiviral particles (TL506284V, ORIGENE) were injected into the vein. The following week, gemcitabine (10 mg/kg) and ferrostatin-1 (1 mg/kg) were intraperitoneally injected three times a week for 14 days. On the 14th day, the mice were euthanized.

The tumors were harvested, weighed, and fixed in 4% paraformaldehyde. Metastases were photographed. Tumor volume was measured using calipers and calculated using the following formula = $0.5 \times \text{length} \times \text{width}^2$. All animal experimental procedures followed the National Institutes of Health Guide for the Care and Use of Laboratory Animals and were performed in accordance with protocols approved by the Institutional Animal Care and Use Committee of the Seoul Yonsei Pharmaceutical University Experimental Animal Center (approval #2019-0104).

16. Statistical analysis

Statistical analyses were performed using one-way or two-way analysis of variance (ANOVA) in GraphPad Prism version 8.0. Data are presented as mean \pm standard deviation. Statistical significance was indicated (*P < 0.05; **P < 0.01; ***P < 0.001; #P < 0.05; ##P < 0.01; ###P < 0.001).

III. RESULTS

1. SLC38A5 correlates with gemcitabine-resistance pancreatic cancer patients

To investigate SLC38A5 expression in pancreatic cancer cells, I analyzed mRNA and protein levels in human pancreatic cancer cell lines. I confirmed that expression of SLC38A5 in five PDAC cell lines (Aspc-1, Bxpc-3, Capan-1, PANC-1, and MIA PaCa-2) using RT-PCR and western blot analysis (Figure. 1A). I examined the expression of SLC38A5 in pancreatic cancer using RT-PCR, western blotting, and immunohistochemical staining. Based on these experiments, I found that pancreatic tumor tissues have higher expression levels of SLC38A5 than normal tissues (Figure. 1B and C). Moreover, increased levels of SLC38A5 tended to decrease the overall survival (OS) and disease-specific survival (DSS) of patients with pancreatic cancer (Figure. 1D and E).

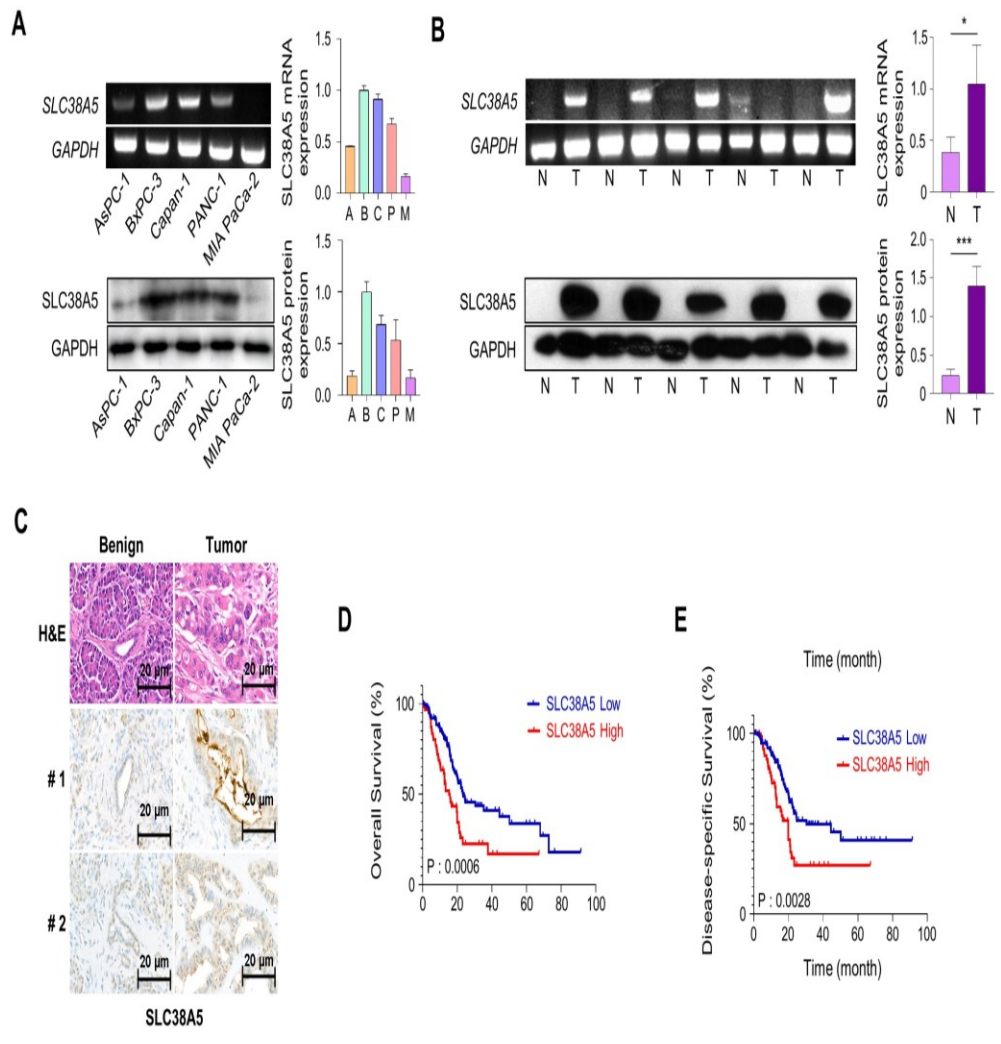
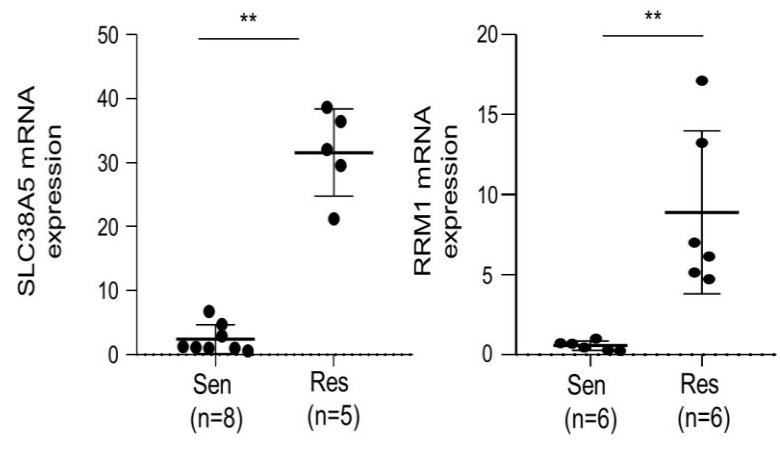


Figure 1. Expression of SLC38A5 in pancreatic cancer. (A) mRNA and protein expression of SLC38A5 in pancreatic cancer cell lines. (B) mRNA and protein expression of SLC38A5 in normal tissues and pancreatic cancer tissues. (C) H&E staining of the SLC38A5 in tumor tissue. (D) Kaplan-Meier analysis for overall survival between SLC38A5 high group and low group. (E) Kaplan-Meier analysis for disease-specific survival between SLC38A5 high group and low group. Bars represent means \pm SD. *, $P < 0.05$; **, $P < 0.01$; ***, $P < 0.001$.

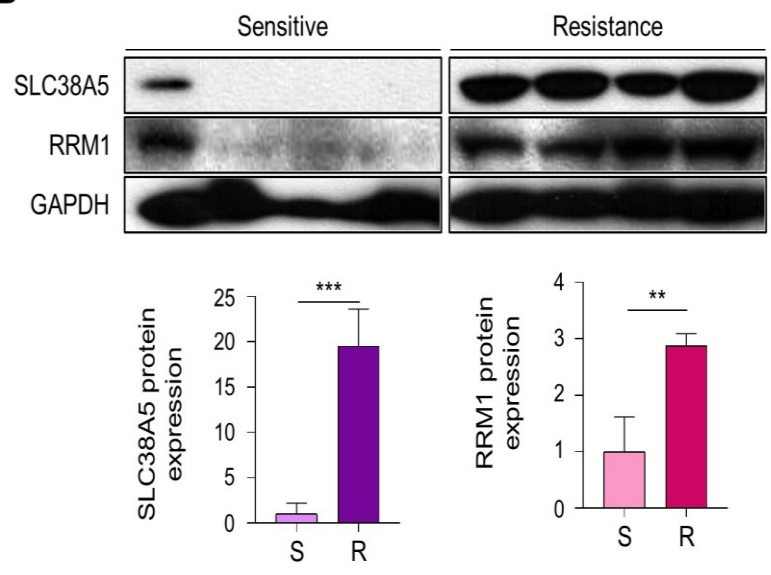
2. SLC38A5 correlates with gemcitabine-resistance in pancreatic cancer

To verify whether SLC38A5 and gemcitabine-resistance are significantly correlated, I confirmed the mRNA expression levels of SLC38A5, RRM1, a widely recognized gemcitabine resistant marker, in both gemcitabine-sensitive and gemcitabine-resistant patient samples^{22,23}. Both SLC38A5 and RRM1 mRNA levels were higher in gemcitabine-resistant pancreatic cancer tissues than in gemcitabine-sensitive patient tissues (Figure. 2A). Similarly, the protein levels of both SLC38A5 and RRM1 were increased in drug-resistant pancreatic cancer patients compared to those in the drug-sensitive group (Figure. 2B). I hypothesized that SLC38A5 is overexpressed in gemcitabine-resistant conditions and plays an important role in the regulation of gemcitabine-resistant environments. To elucidate the role of SLC38A5 in gemcitabine-resistance, I established gemcitabine-resistant pancreatic cancer cell lines using PANC-1 and Capan-1 cells (PANC-GR and Capan-GR, respectively) by confirming the half-maximal inhibitory concentration (IC_{50}) via a cell viability test (Figure. 2C and D). However, the expression of SLC38A5 was not increased in the other GR cell lines (Aspc-1, Bxpc-3 and MIA PaCa-2). Consistent with previous results, higher SLC38A5 and RRM1 expression was confirmed at the mRNA and protein levels in the gemcitabine-resistant cell lines than in the gemcitabine-sensitive cell lines (Figure. 2E).

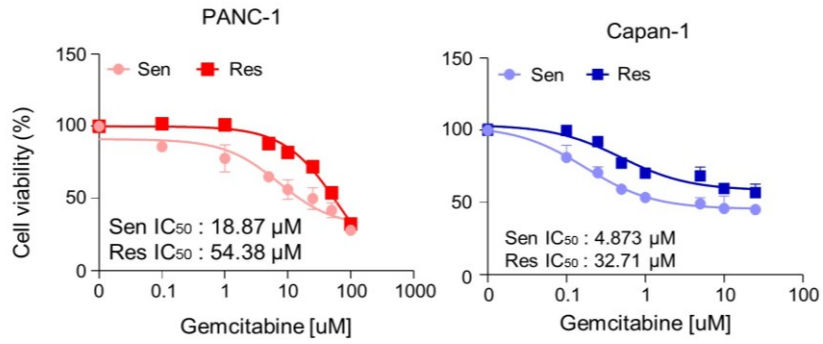
A



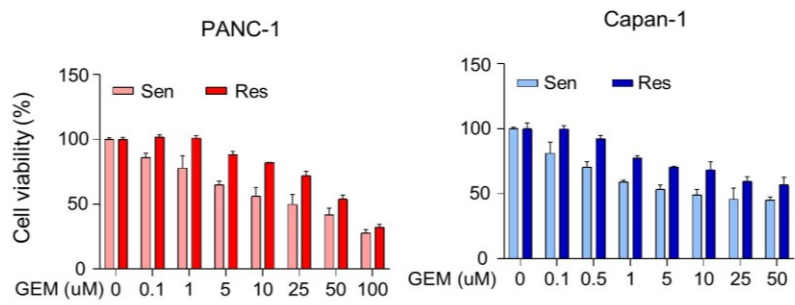
B



C



D



E

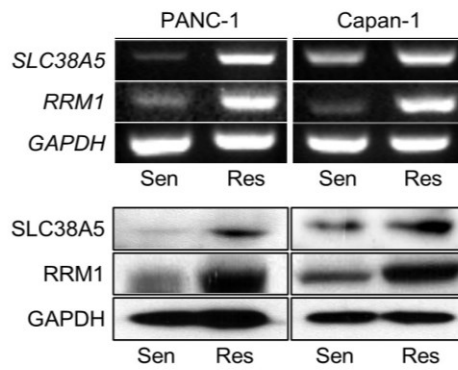
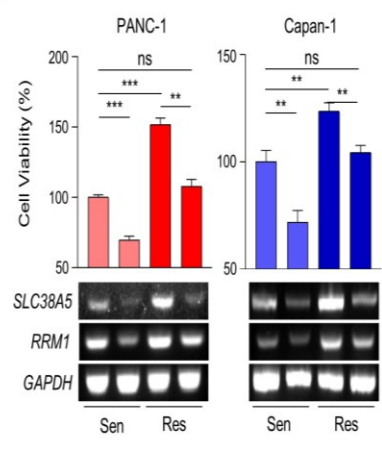


Figure 2. SLC38A5 correlates with gemcitabine-resistance in pancreatic cancer. (A) Dot plot of SLC38A5 and RRM1 gene expression level in purified mRNA from gemcitabine sensitive and resistance pancreatic cancer patient tissue. (B) Protein expression of SLC38A5 and RRM1 between gemcitabine sensitive and resistance pancreatic cancer patient tissue. (C) Median inhibitory concentration (IC₅₀) values of gemcitabine for each cell line (PANC-1 and Capan-1). (D) Cell viability of PANC-1, PANC-GR, Capan-1 and Capan-GR is determined using the WST assay. Each cell lines transfected with siSLC38A5. Transfection is confirmed via RT-PCR. (E) mRNA and protein expression of SLC38A5 and RRM1 in gemcitabine-sensitive PDAC cell lines (PANC-1 and Capan-1) and gemcitabine-resistance PDAC cell lines (PANC-GR and Capan-GR). Bars represent means \pm SD. ns = not significant; **, P < 0.01; ***, P < 0.001.

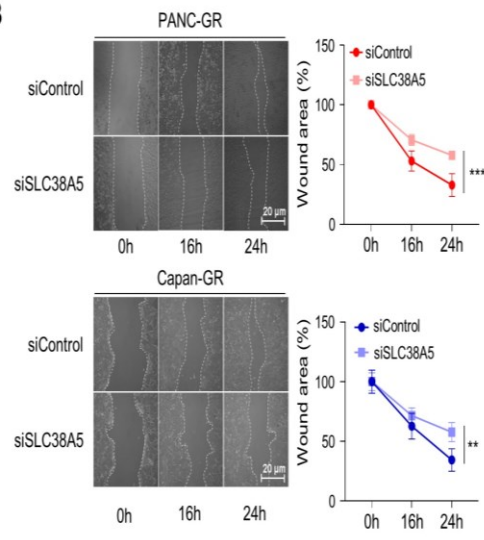
3. Deletion of SLC38A5 down-regulates cell viability and migration in gemcitabine-resistance pancreatic cancer cells

To investigate whether SLC38A5 modulates the sensitivity of GR cell lines to gemcitabine, a WST assay was performed in the presence of gemcitabine (10 μ M). Gemcitabine-resistant cells were more proliferative than gemcitabine-sensitive cells. Conversely, when SLC38A5 was deleted in both sensitive and resistant cells, each cell type showed decreased proliferation according to both cell viability and RT-PCR (Figure. 3A). Previous studies have shown that gemcitabine-resistant pancreatic cancer cells show increased levels of both migration and invasion compared to gemcitabine-sensitive cells^{24,25}. However, it remains unclear whether SLC38A5 plays a significant role in cancer metastasis. Knockdown of SLC38A5 expression hindered both the migration and invasion abilities of cancer cells in the wound healing and transwell invasion assays (Figure. 3B and C). To verify whether SLC38A5 controls epithelial-to-mesenchymal transition (EMT), I confirmed EMT-related genes by regulating SLC38A5 mRNA and protein expression in GR cell lines. E-cadherin, an epithelial marker, increased in SLC38A5 knockdown cells. Conversely, the expression of N-cadherin, a mesenchymal marker, decreased (Figure. 3D and E). I also analyzed the gene set enrichment analysis (GSEA) results using RNA sequencing data. Therefore, I confirmed that SLC38A5 is involved in the proliferation and EMT of gemcitabine-resistant pancreatic cancer cells (Figure. 3F).

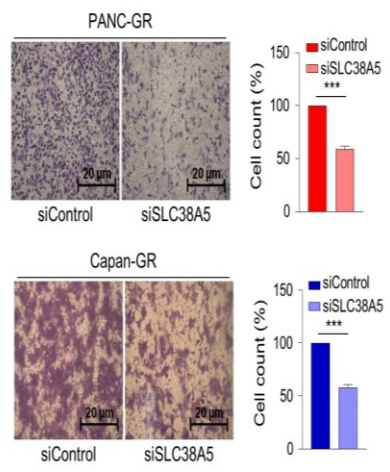
A



B



C



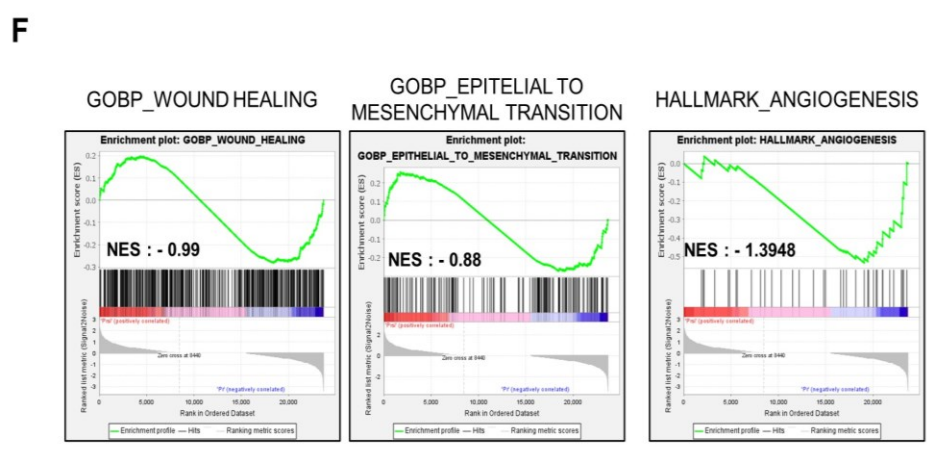
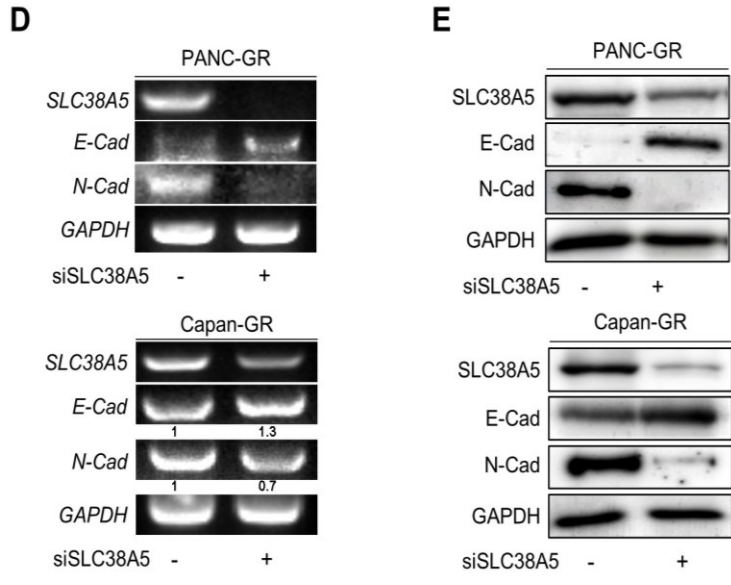
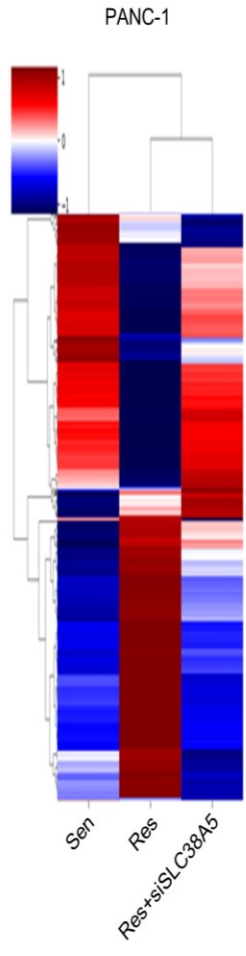


Figure 3. Deletion of SLC38A5 down-regulates cell viability and migration in gemcitabine-resistance pancreatic cancer cells. (A) Cell viability of PANC-1, PANC-GR, Capan-1 and Capan-GR is determined using the WST assay. Each cell lines transfected with siSLC38A5. Transfection is confirmed via RT-PCR. (B) Migration of cells is measured with wound healing assay. The statistical analysis of wound closure percentage is measured by Image J software. (C) Representative photographs of the number of invaded cells that pass through the Matrigel-coated Transwell invasion assay. (D) and (E) The EMT marker expression of siRNA transfected PANC-GR and Capan-GR is analyzed by RT-PCR (F), and western blot (G). (F) GSEA for significant enrichment for wound healing, EMT and angiogenesis. Bars represent means \pm SD. ns = not significant; **, $P < 0.01$; ***, $P < 0.001$.

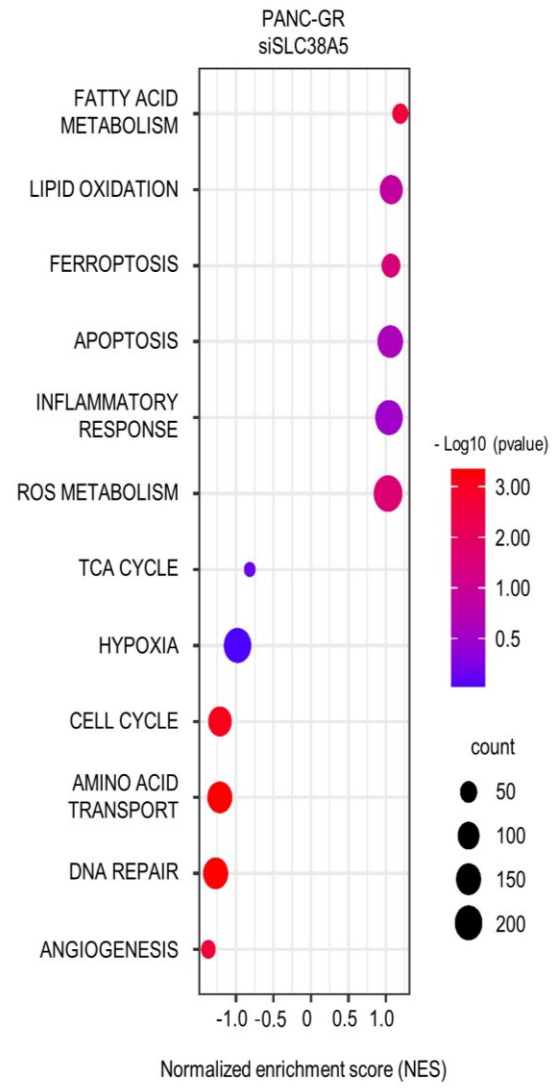
4. Inhibition of SLC38A5 induces changes in ferroptosis-regulating genes

Next, I performed RNA sequencing to determine whether SLC38A5 plays a crucial role in any biological mechanism in gemcitabine-resistant cells. Using heat map data, I identified various differential genes compared among PANC-1, PANC-GR, and PANC-GR cells with SLC38A5 knockdown (Figure. 4A). Using the DAVID analysis tool, a bubble plot showed that inhibition of SLC38A5 upregulated ferroptosis and lipid oxidation (Figure. 4B). Furthermore, the TCA cycle, hypoxia, and cell cycle pathways are downregulated^{26,27}. Additionally, I analyzed the inhibition of SLC38A5 in promoting ferroptosis through the GSEA graph for both PANC-GR and Capan-GR (Figure. 4C). Ferroptosis is a programmed cell death pathway associated with lipid ROS. I performed a correlation analysis of the expression of SLC38A5 and ferroptosis-related genes. I found that SLC7A11 and FTH, ferroptosis-inhibiting genes, were positively correlated with SLC38A5, whereas ACSL4 and ALOX12, ferroptosis-inducing genes, were negatively correlated with SLC38A5^{28,29} (Figure. 4D). Also, I examined the similar results via q-PCR analysis compared among PANC-1, PANC-GR, and PANC-GR with SLC38A5 knockdown (Figure. 4E). Collectively, I found that SLC38A5 inhibition in PANC-GRs induced lipid ROS and ferroptosis. I believe that the results of this study will play an important role in overcoming gemcitabine-resistance.

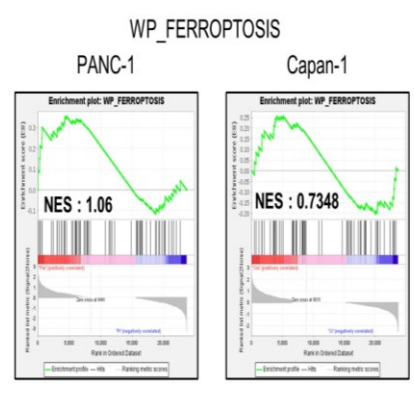
A



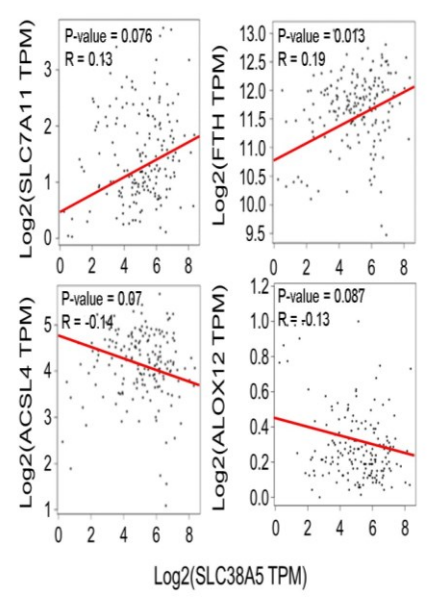
B



C



D



E

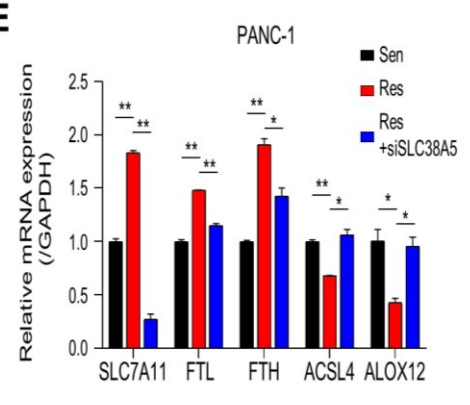


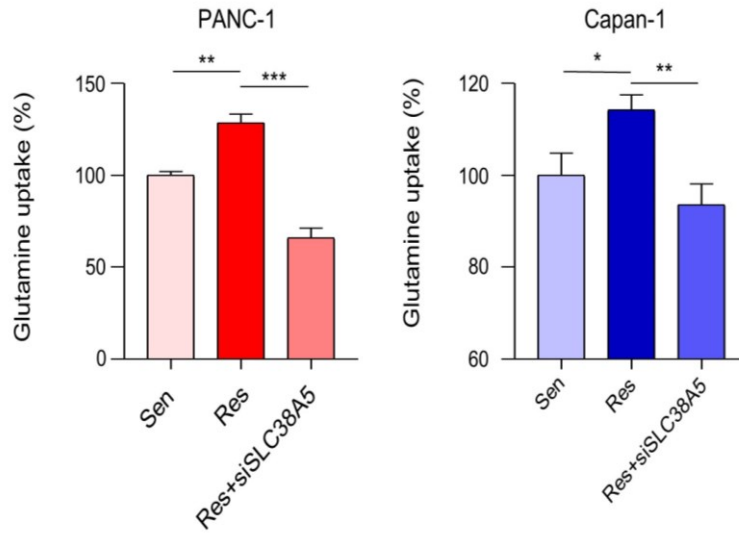
Figure 4. Inhibition of SLC38A5 induces changes in ferroptosis-regulating genes.

(A) Heat map analysis of distribution of genes from PANC-1, PANC-GR, and PANC-GR with siSLC38A5 cells. (B) DAVID-based gene ontology bubble plot analysis of mRNA sequencing results from PANC-GR and PANC-GR with siSLC38A5 cells. (C) Gene Set Enrichment Analysis (GSEA) for significant enrichment for ferroptosis. (D) Correlation analysis of SLC38A5 and ferroptosis-related genes in pancreatic cancer. (E) mRNA levels of the ferroptosis-related genes were quantified by qPCR in PANC-1, PANC-GR and PANC-GR with siSLC38A5. Bars represent means \pm SD. *, $P < 0.05$; **, $P < 0.01$.

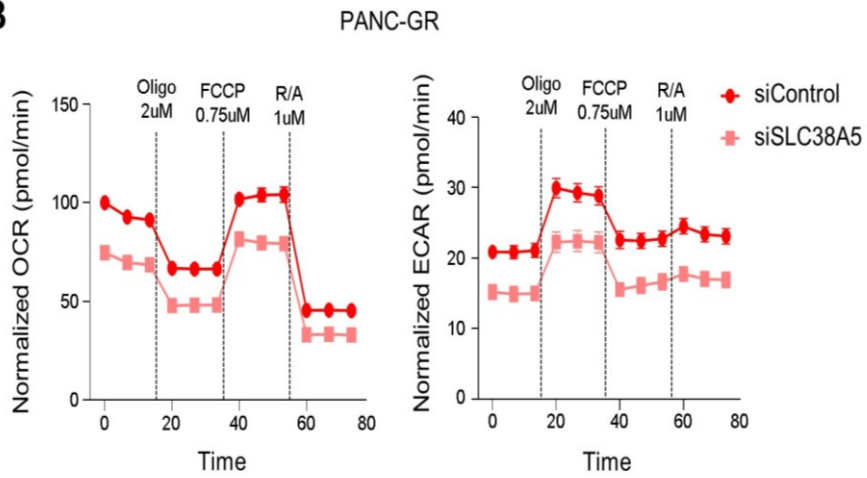
5. SLC38A5 regulates glutathione synthesis and related genes

Cancer cells, specifically drug-resistant cells, rely more on nutrients than normal cells because of their rapid cell proliferation and migration. Glutamine is the main fuel used by cancer cells. Therefore, I examined whether SLC38A5 regulates glutamine consumption in gemcitabine-resistant cells using a glutamine assay kit. I found that the glutamine consumption rate was much higher in gemcitabine-resistant cells (PANC-GR and Capan-GR) than in gemcitabine-sensitive cells (PANC-1 and Capan-1). Additionally, its rate was downregulated when SLC38A5 was silenced (Figure. 5A). When glutamine enters cells, it is involved in mitochondrial functions, such as the TCA cycle, is converted to glutamate through glutaminolysis, and is then released from the mitochondria¹³. Therefore, I measured the oxygen consumption rate (OCR) and extracellular acidification rate (ECAR) using a Seahorse XF24 extracellular flux analyzer to confirm mitochondrial activity. Both OCR and ECAR levels were lower in PANC-GR cells with SLC38A5 deletion (Figure. 5B). Additionally, GSEA showed that the inhibition of SLC38A5 reduced mitochondrial activity (Figure. 5C). The presence of glutamate in cells contributes to GSH synthesis³⁰. Glutathione is a key factor in the ROS levels related to ferroptosis³¹. Using a glutathione assay kit, glutathione levels were found to be higher in gemcitabine-resistant cells than in gemcitabine-sensitive cells. Conversely, when SLC38A5 was suppressed, glutathione levels decreased (Figure. 5D). I further confirmed that the GSH-related genes NRF2 and GPX4 were upregulated in GR cells (PANC-GR and Capan-GR) and downregulated in GR cells transfected with siSLC38A5 by RT-PCR and western blotting (Figure. 5E and F).

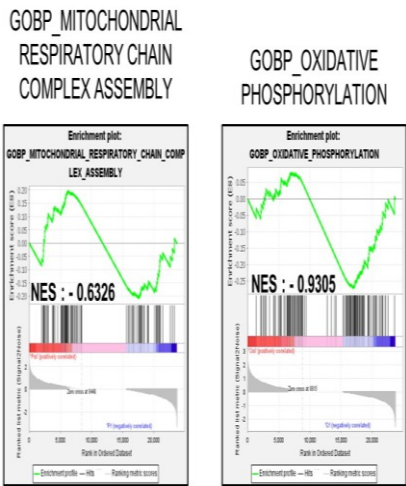
A



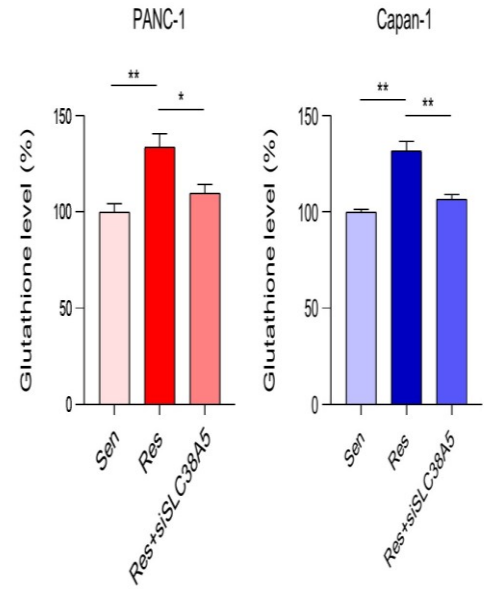
B



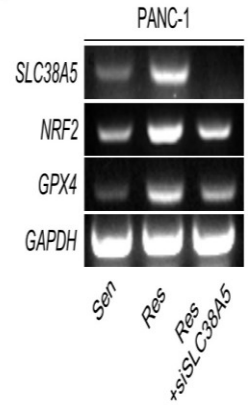
C



D



E



F

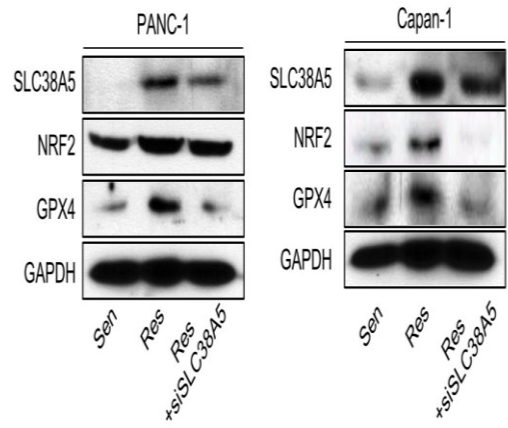
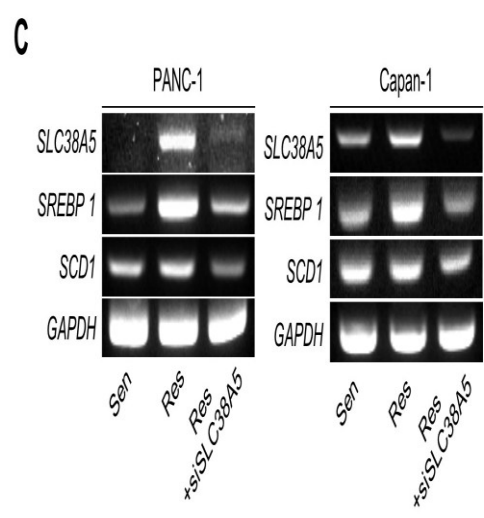
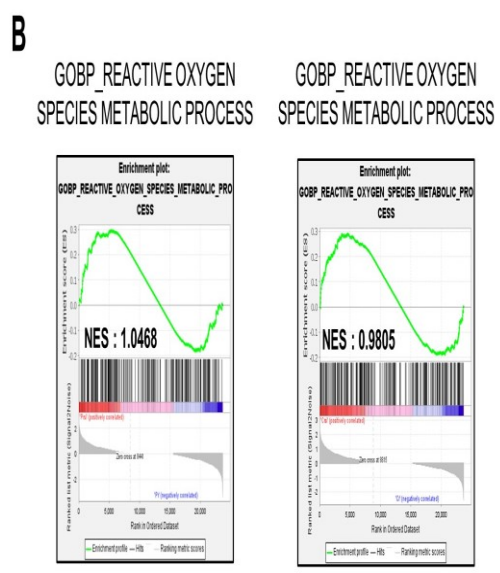
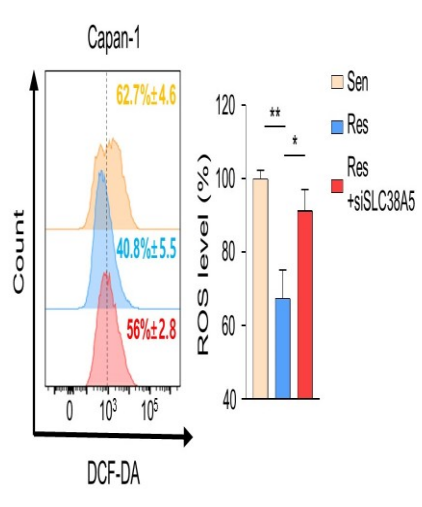
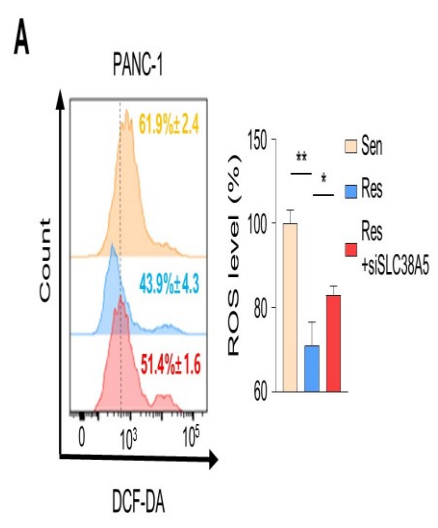


Figure 5. SLC38A5 regulates glutathione synthesis and related genes. (A) Comparison of glutamine uptake. (B) Oxygen consumption rate (OCR) is determined and calculated under oligomycin, carbonyl cyanide p-(trifluoromethoxy) phenylhydrazone (FCCP), and Rot/antimycin A treatments. Data represents the mean \pm SD (n=3). (C) GSEA for significant enrichment for mitochondrial activity. (D) Comparison of glutathione level. (E) and (F) Expression of glutathione-related genes is analyzed by RT-PCR (E) and western blot (F). Bars represent means \pm SD. *, $P < 0.05$; **, $P < 0.01$; ***, $P < 0.001$.

6. SLC38A5 modulates lipid ROS through GSH-mediated ROS and mTOR-SREBP1 signaling in gemcitabine-resistance pancreatic cancer cells

To investigate whether SLC38A5 regulates intercellular ROS levels, I performed fluorescence-activated cell sorting (FACS) analysis using DCF-DA staining by manipulating the expression levels of SLC38A5 in GR cell lines. I observed that ROS levels were much lower in gemcitabine-resistant cell lines than in gemcitabine-sensitive cell lines. As SLC38A5 expression decreased, ROS levels also increased. (Figure. 6A). Based on the previous results from FACS analysis, I also confirmed by GSEA that ROS levels increased when SLC38A5 expression levels were suppressed. (Figure. 6B). Previous studies have reported that glutamine uptake leads to upregulation of the mTOR-SREBP1 signaling pathway, which regulates lipid ROS¹⁶. SREBP1 (sterol regulatory element-binding protein 1) is one of the proteins regulating lipid metabolism and acts as a transcription factor for lipid synthesis-related genes such as FASN, ACLY, and SCD1³². Recent studies have demonstrated that SCD1 accumulates monounsaturated fatty acids (MUFAs), which suppress and inhibit ferroptosis^{17,33}. Both the mRNA and protein levels of SREBP1 and SCD1 were increased in gemcitabine-resistant cells and were downregulated when SLC38A5 was silenced (Figure. 6C and D). Prior to this experiment, I confirmed that mTOR phosphorylation was reduced in a glutamine-deficient environment by culturing cells in glutamine-free media. To determine whether SLC38A5 significantly regulates ferroptosis by controlling lipid ROS levels, I measured lipid ROS levels in gemcitabine-resistant cell lines by manipulating SLC38A5 expression via FACS analysis with staining BODIPY-C11. As a result, lipid ROS levels were decreased in gemcitabine-resistant cells but were stored when SLC38A5 expression levels were inhibited (Figure. 6E). Gemcitabine induces apoptosis; however, this apoptotic effect is weakened under gemcitabine-resistant conditions^{34,35}. To investigate whether SLC38A5 regulates apoptosis, I measured the mRNA expression levels of apoptosis-related genes in

PANC-GR cells. PANC-GR showed more anti-apoptotic effects than PANC-GS based on the downregulated levels of BAX, caspase 3, and caspase 9 than PANC-GS. Conversely, the mRNA levels of the apoptosis-inducing genes were upregulated when SLC38A5 was silenced (Figure. 6F). Thus, glutamine uptake through SLC38A5 ultimately suppresses lipid ROS production through the GSH-mediated ROS and mTOR-SREBP1 signaling pathway in gemcitabine-resistant cells, leading to apoptosis.



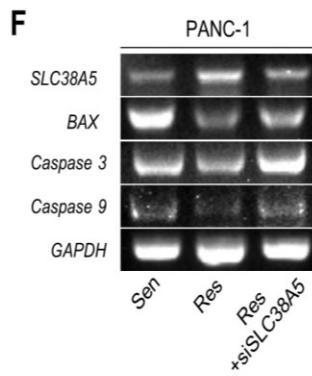
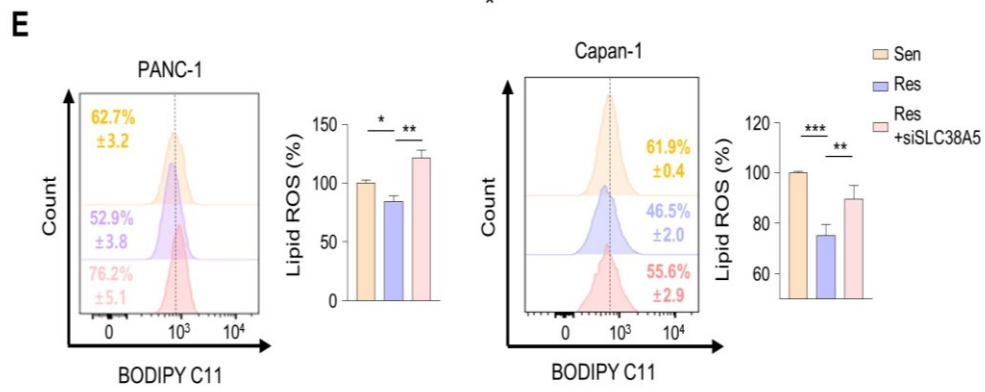
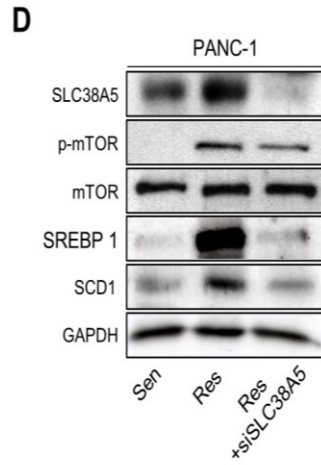
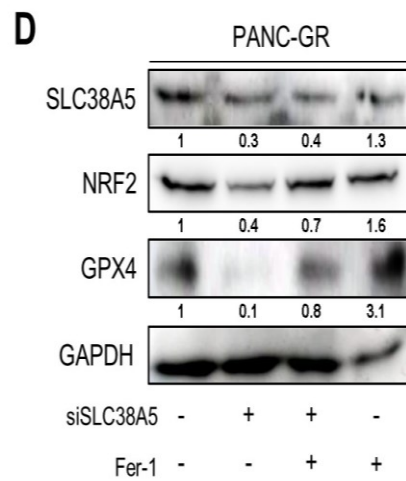
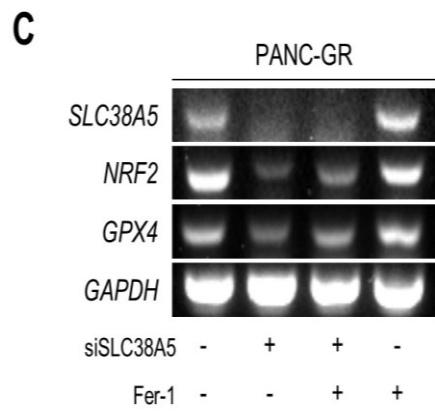
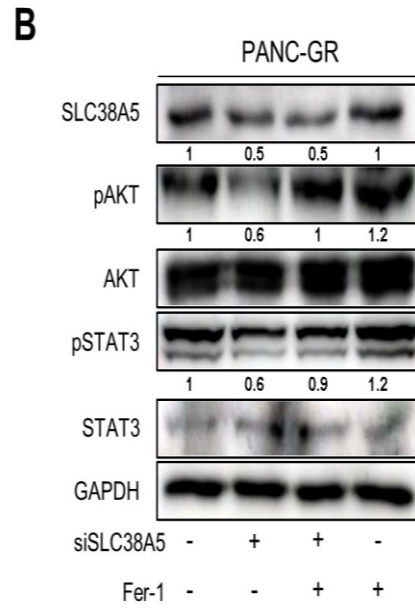
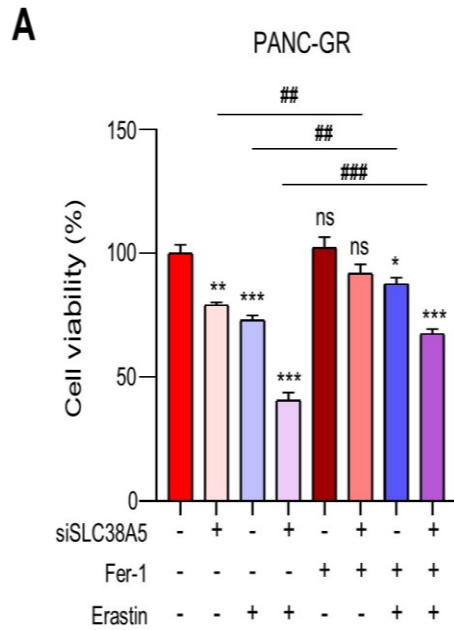


Figure 6. SLC38A5 modulates lipid ROS through GSH-mediated ROS and mTOR-SREBP1 signaling in gemcitabine-resistance pancreatic cancer cells. (A) Relative ROS production was measured using flow cytometry after dichlorofluorescein (DCF)-staining. Bar graph was analyzed by Image J software. (B) GSEA for significant enrichment for ROS level. (C) and (D) Expression of mTOR-SREBP1 signaling genes was analyzed by RT-PCR (C), and western blot (D). (E) Flow cytometry analysis of lipid ROS. Bars graph is analyzed by Image J software. (F) mRNA levels of apoptosis-related genes in PANC-1, PANC-GR and PANC-GR with siSLC38A5. Bars represent means \pm SD. *, $P < 0.05$; **, $P < 0.01$; ***, $P < 0.001$.

7. Inhibition of SLC38A5 induces ferroptosis in gemcitabine-resistance pancreatic cancer cells

To validate whether SLC38A5 directly regulates ferroptosis, I used ferrostatin-1 as a ferroptosis inhibitor. Inhibition of SLC38A5 sensitized PANC-GR cells to gemcitabine (Figure. 3A); however, their viability was rescued when ferrostatin-1 was applied to PANC-GR cells, even in the presence of Erastin, a ferroptosis inducer. (Figure. 7A). With respect to the cell proliferation, I also confirmed that cell proliferation-related genes were upregulated when ferroptosis was inhibited (Figure. 7B). I also utilized NRF2 and GPX4 as antioxidant markers to verify whether ferrostatin-1 could regulate when GR cells expression a low level of SLC38A5 at both mRNA and protein levels. I confirmed that ferrostatin-1 increased the antioxidant levels (Figure. 7C and D). Using wound healing and invasion assays, I also confirmed that ferrostatin-1 attenuated the EMT effect of siSLC38A5 in PANC-GR cells (Figure. 7E and F). Moreover, ferrostatin-1 inhibits ferroptosis by inhibiting lipid ROS^{36,37}. Consistent with previous studies, my results showed that ferrostatin-1 inhibited both ROS and lipid ROS production (Figure. 7G and H). Therefore, the anti-proliferative, EMT, ROS, and ferroptotic effects mediated by SLC38A5 inhibition could be prevented when ferroptosis is suppressed.



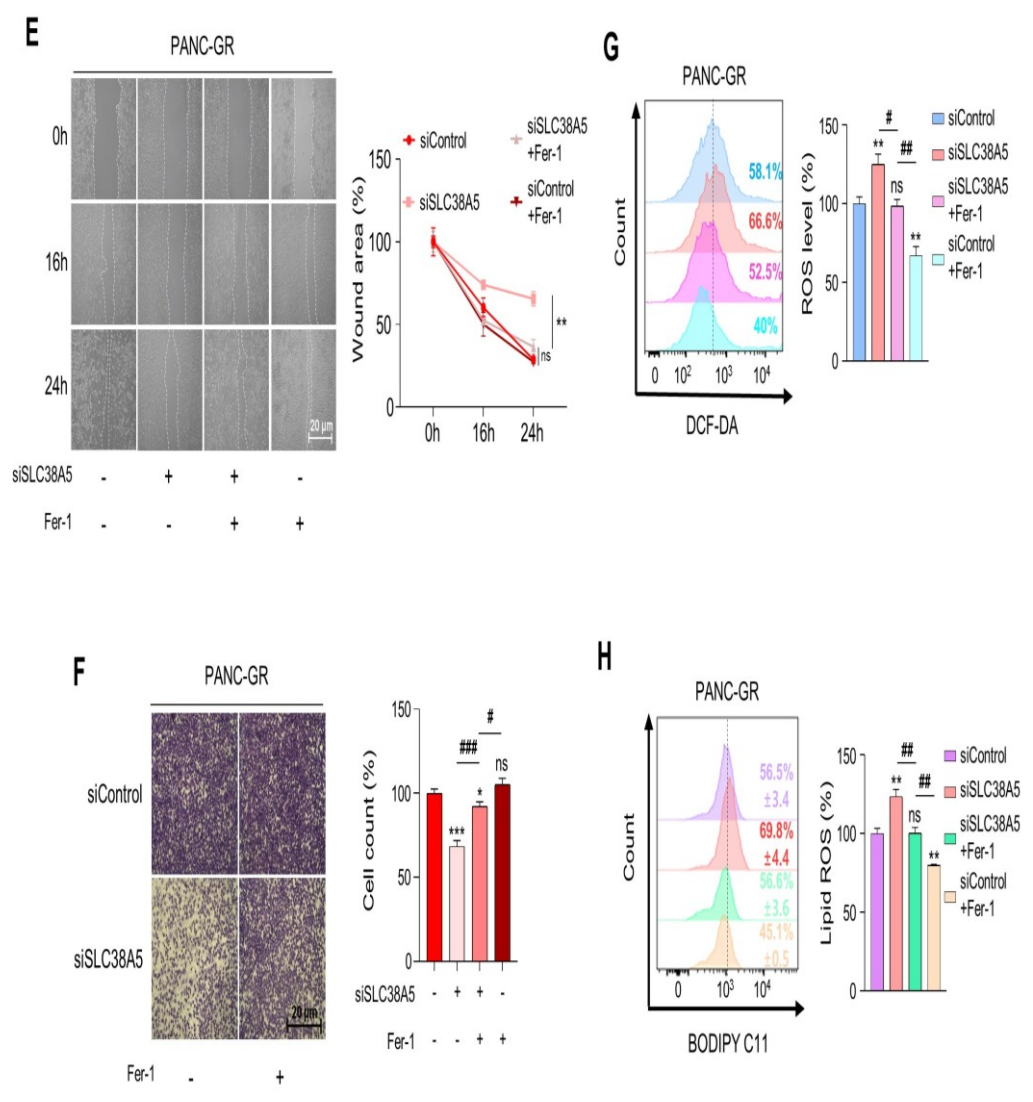


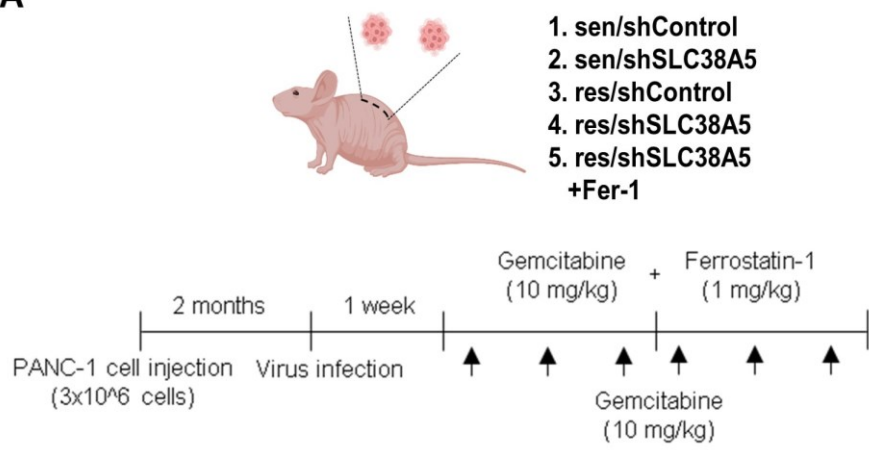
Figure 7. Inhibition of SLC38A5 induces ferroptosis in gemcitabine-resistance pancreatic cancer cells. (A) WST assay is performed to determine cell viability using indicated PANC-GR groups. (B) Cell proliferation marker is confirmed via western blot. (C) and (D) Expression of glutathione-related genes is measured by RT-PCR (C) and western blot (D). (E) and (F) Migration of cell is measured through wound healing assay (E) and Matrigel-coated transwell invasion assay (F). (G) Relative ROS production in indicated PANC-GR groups was measured via FACS analysis. (H) FACS analysis of lipid ROS in indicated PANC-GR groups. Bar graph is analyzed by Image J software. Ferrostatin-1 (Fer-1) is treated with 20 uM. Bars represent means \pm SD. ns = not significant; *, $P < 0.05$; **, $P < 0.01$; ***, $P < 0.001$.

8. Knockdown of SLC38A5 suppress tumor growth and metastasis *in vivo*

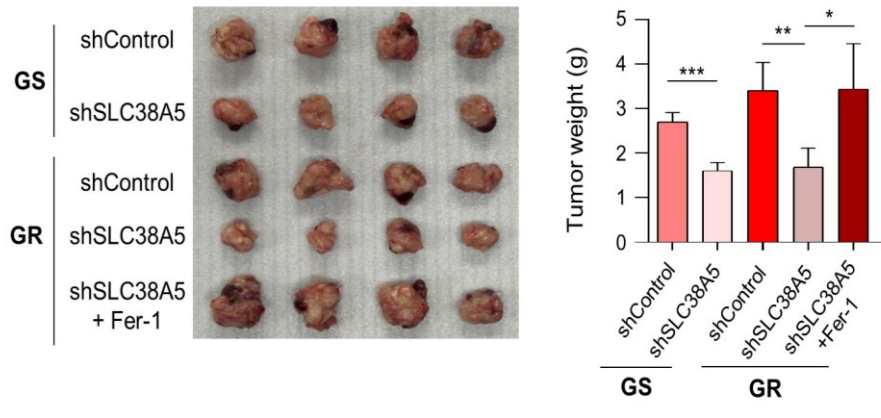
To evaluate whether SLC38A5 plays an important role in the metastasis of gemcitabine-resistant pancreatic tumors *in vivo*, I generated a BALB/c nude mouse model bearing orthotopic tumors. After 2 months, gemcitabine and ferrostatin-1 were intraperitoneally injected at the indicated concentrations three times a week for 2 weeks (Figure. 8A). After drug injection, each group exhibited significantly different tumor sizes. The gemcitabine-resistant group had a much larger tumor size than the gemcitabine-sensitive group. Moreover, inhibition of SLC38A5 hindered tumor growth in both the gemcitabine-sensitive and gemcitabine-resistant groups. Furthermore, treatment with ferrostatin-1 increased tumor size and weight (Figure. 8B). Expression levels of SLC38A5, EMT markers, and ferroptosis markers were reduced in the tumor and livers of the knockdown group in accordance with the *in vitro* results; the treatment of Ferrostatin-1, however, negated the effect of the knockdown (Figure 8C). Western blot revealed the same trend in protein expressions in the tumors as well (Figure 8D). Furthermore, the gemcitabine-resistant group showed liver metastases, whereas the gemcitabine-resistant with SLC38A5 knock-down group showed no liver metastases. Conversely, the inhibition of ferroptosis-induced liver metastasis by preventing SLC38A5 inhibition (Figure. 8E).

Collectively, SLC38A5 inhibition sensitizes drug-resistant pancreatic cancer cells to gemcitabine by inducing ferroptosis and suppressing tumor growth and metastasis. Therefore, targeting SLC38A5 may play a major role in improving the 5-year survival rate of patients with pancreatic cancer and overcoming chemoresistance in pancreatic cancer for clinical purposes. Together, these results demonstrated that SLC38A5 regulates ferroptosis in gemcitabine-resistant pancreatic cancer *in vitro* and *in vivo* (Figure. 9).

A



B



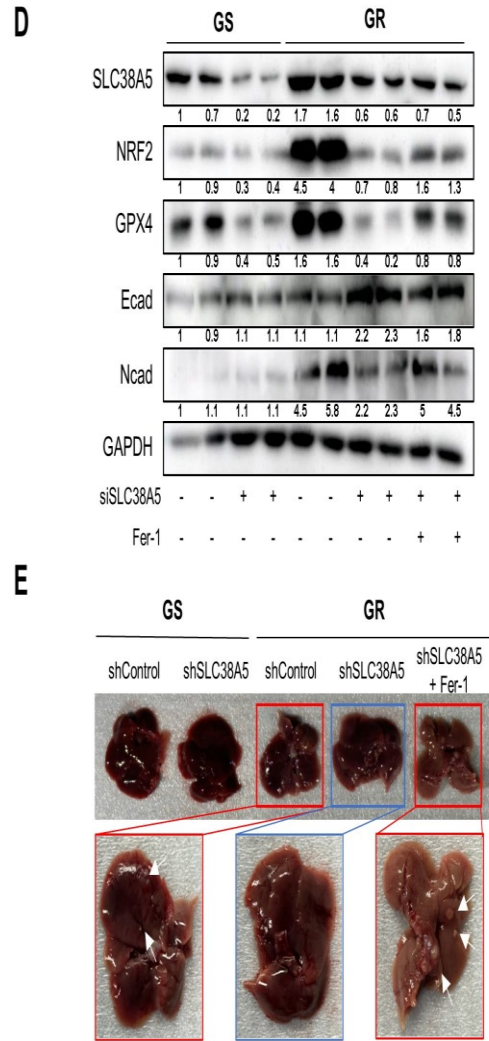
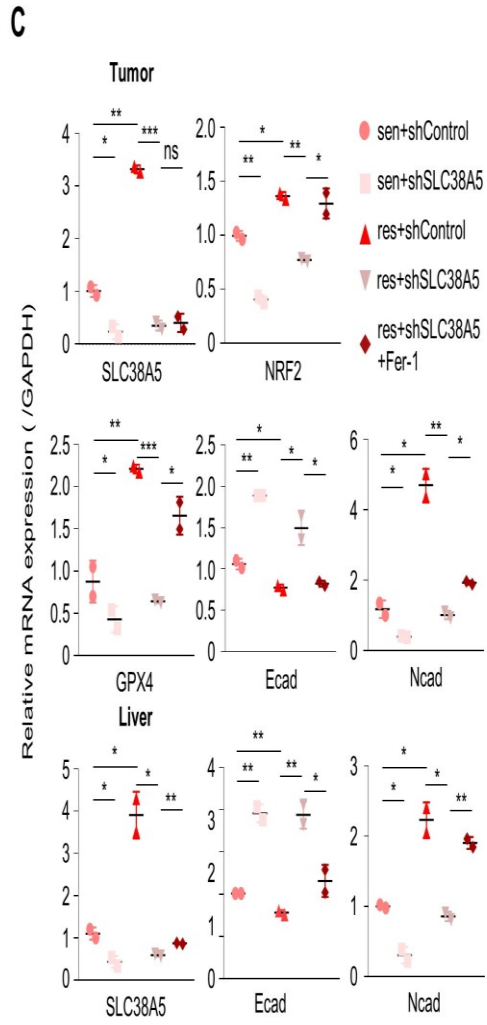


Figure 8. Knockdown of SLC38A5 suppress tumor growth and metastasis in vivo.

(A) Schematic of mouse experimental grouping and processing of the orthotopic model. (B) Images and weights of the tumors harvested from mice. (C) mRNA levels of the EMT and ferroptosis-related genes in tumors and livers were quantified by qPCR. (D) Protein expression of EMT and ferroptosis-related genes in tumors. (E) Liver metastasis images. All experiments were performed at least three times. Bars represent means \pm SD. ns = not significant; *, $P < 0.05$; **, $P < 0.01$; ***, $P < 0.001$.

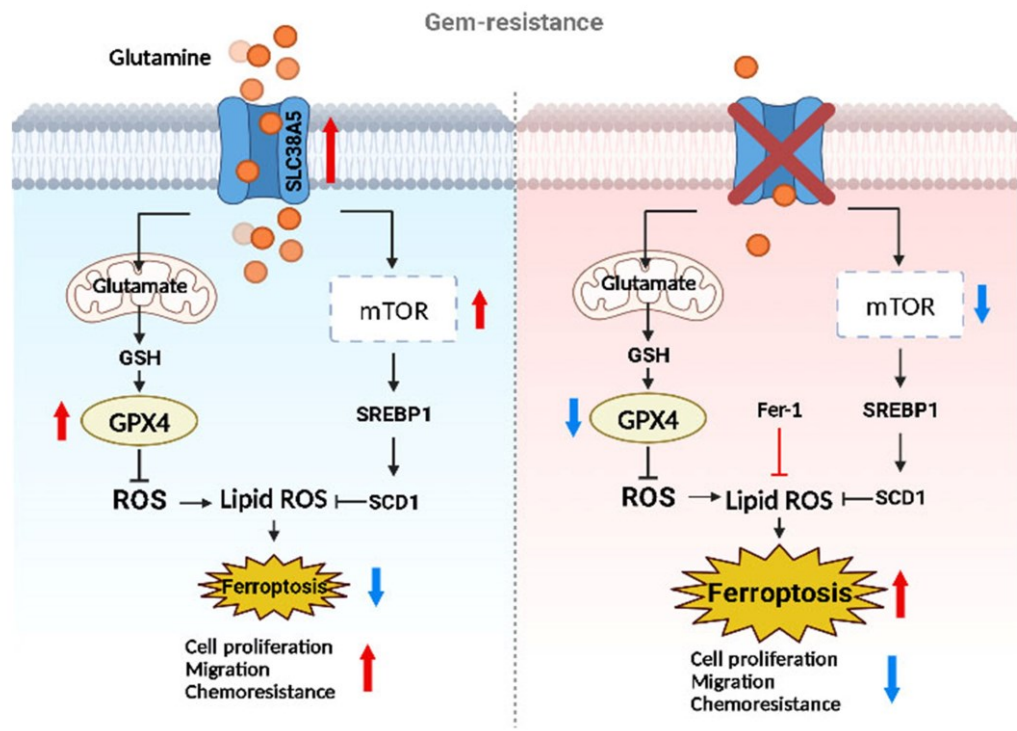


Figure 9. The graphical abstract illustrates the regulatory mechanism of SLC38A5 in gemcitabine-resistance pancreatic cancer.

IV. DISCUSSION

Pancreatic cancer is one of the most fatal diseases with one of the highest mortality rates among all major cancers³⁸. Despite the development of many treatments and diagnostic methods, the poor prognosis of pancreatic cancer has not improved compared with that of other cancers. Although gemcitabine is known as a standard drug for the treatment of PDAC, it has a major limitation in that drug resistance can easily develop. Therefore, the present study aimed to overcome gemcitabine-resistance in pancreatic cancer.

SLC38A5 is a well-known amino acid transporter that transport glutamine⁸. Recent studies have shown that glutamine plays a critical role in the growth, survival, and drug resistance of pancreatic cancer³⁹. Glutamine is a key nutrient that promotes drug resistance in breast cancer⁴⁰. However, the mechanism through which glutamine affects drug resistance in pancreatic cancer has not yet been elucidated. In this study, I investigated the mechanism by which glutamine regulates gemcitabine-resistance. A previous study has shown that glutamine is transported into the mitochondria and converted into glutamate via glutaminolysis. It is also involved in GSH synthesis¹¹. I confirmed that glutamine uptake and glutathione levels were increased in gemcitabine-resistant PDAC cells and decreased when SLC38A5 was silenced (Figure. 4A and D), suggesting that glutamine transported by SLC38A5 contributes to glutathione synthesis in PDAC cells. Synthesized glutathione regulates intracellular ROS levels by modulating the related genes NRF2 and GPX4. Many studies indicate that reduced ROS levels may also induce gemcitabine-resistance and are characteristic of gemcitabine-resistance^{41,42}. I also confirmed reduced ROS levels in gemcitabine-resistant PDAC cells (PANC-GR) using FACS analysis. Conversely, the ROS levels increased when SLC38A5 was inhibited (Figure. 4G).

Several studies have demonstrated that glutamine increases mTOR activity through phosphorylation in cancer cells¹⁶. I found that phosphoryl-mTOR was upregulated in

gemcitabine-resistant PDAC cells compared to that in sensitive cells and was downregulated when SLC38A5 was inhibited (Figure. 4J). SREBP1 is known to be involved in fatty acid synthesis and is a downstream target of mTOR⁴³. SREBP1 and SCD1 are inhibitory markers of ferroptosis because they convert polyunsaturated fatty acids (PUFAs), which trigger lipid oxidation, to MUFAs³³. I showed that the mTOR-SREBP1-SCD1 pathway was upregulated in gemcitabine-resistant PDAC cells but decreased when SLC38A5 was silenced (Figure. 4I and J). Lipid ROS production is known to be mediated by several pathways⁴⁴. I elucidated the lipid ROS levels through two pathways: the GSH-mediated ROS level and the mTOR pathway. I validated that lipid ROS are downregulated in gemcitabine-resistant PDAC cells compared to gemcitabine-sensitive cells. Furthermore, lipid ROS levels increased when SLC38A5 was silenced (Figure. 4K).

Ferroptosis is a type of cell death triggered by the accumulation of lipid ROS¹⁸. My results indicate that SLC38A5 deletion results in the accumulation of lipid ROS in gemcitabine-resistant PDAC cells. In the present study, I used ferrostatin-1, which inhibits ferroptosis by preventing lipid ROS production. As hypothesized, ferrostatin-1 treatment had the opposite effect on SLC38A5 inhibition in gemcitabine-resistant PDAC cells (Figure. 5). Based on my previous results, I showed that suppression of ferroptosis in gemcitabine-resistant PDAC cells was triggered by SLC38A5 inhibition.

In Conclusion, upregulation of SLC38A5 in gemcitabine-resistant PDAC cells increased the viability and invasive ability of gemcitabine-resistant PDAC cells compared to sensitive cells by upregulating glutamine uptake. SLC38A5 significantly reduces ferroptosis through inhibition of lipid ROS accumulation in gemcitabine-resistant PDAC cells. However, SLC38A5 silencing in gemcitabine-resistant PDAC cells reduced cell proliferation and EMT and induced ferroptosis. These mechanistic changes eventually increase the sensitivity of cells resistant to gemcitabine. In summary, I believe that targeting SLC38A5 will significantly contribute to the treatment of patients with gemcitabine-resistant pancreatic cancer and improve their 5-year survival rate.

V. CONCLUSION

Overall, my study showed that inhibition SLC38A5 reduced gemcitabine resistance in PDAC. Glutamine uptake due to SLC38A5 inhibition lowered GSH levels and increased intracellular ROS level. Also, deletion of SLC38A5 downregulated mTOR-SREBP1-SCD1 signaling. Inhibition of SLC38A5 increased lipid ROS level and lead to ferroptosis, suppressing tumor growth and metastasis *in vivo*. Therefore, targeting SLC38A5 may be a promising therapeutic agent for improving the survival rate of patients with gemcitabine-resistant pancreatic cancer.

REFERENCES

1. Kaur S, Baine MJ, Jain M, Sasson AR, Batra SK. Early diagnosis of pancreatic cancer: challenges and new developments. *Biomark Med* 2012;6:597-612.
2. Chu LC, Goggins MG, Fishman EK. Diagnosis and Detection of Pancreatic Cancer. *Cancer J* 2017;23:333-42.
3. Ansari D, Tingstedt B, Andersson B, Holmquist F, Stureson C, Williamsson C, et al. Pancreatic cancer: yesterday, today and tomorrow. *Future Oncol* 2016;12:1929-46.
4. Samanta K, Setua S, Kumari S, Jaggi M, Yallapu MM, Chauhan SC. Gemcitabine Combination Nano Therapies for Pancreatic Cancer. *Pharmaceutics* 2019;11.
5. Amrutkar M, Gladhaug IP. Pancreatic Cancer Chemoresistance to Gemcitabine. *Cancers (Basel)* 2017;9.
6. Bhutia YD, Ganapathy V. Glutamine transporters in mammalian cells and their functions in physiology and cancer. *Biochim Biophys Acta* 2016;1863:2531-9.
7. Wang Z, Yemanyi F, Blomfield AK, Bora K, Huang S, Liu CH, et al. Amino acid transporter SLC38A5 regulates developmental and pathological retinal angiogenesis. *Elife* 2022;11.
8. Sniegowski T, Korac K, Bhutia YD, Ganapathy V. SLC6A14 and SLC38A5 Drive the Glutaminolysis and Serine-Glycine-One-Carbon Pathways in Cancer. *Pharmaceutics (Basel)* 2021;14.
9. Ramachandran S, S RS, Sharma M, Thangaraju M, V VS, Sniegowski T, et al. Expression and function of SLC38A5, an amino acid-coupled Na⁺/H⁺ exchanger, in triple-negative breast cancer and its relevance to macropinocytosis. *Biochem J* 2021;478:3957-76.
10. Smith DK, Kates L, Durinck S, Patel N, Stawiski EW, Kljavin N, et al. Elevated Serum Amino Acids Induce a Subpopulation of Alpha Cells to Initiate Pancreatic Neuroendocrine Tumor Formation. *Cell Rep Med* 2020;1:100058.
11. Yoo HC, Yu YC, Sung Y, Han JM. Glutamine reliance in cell metabolism. *Exp Mol Med* 2020;52:1496-516.
12. Hensley CT, Wasti AT, DeBerardinis RJ. Glutamine and cancer: cell biology, physiology, and clinical opportunities. *J Clin Invest* 2013;123:3678-84.
13. Yoo HC, Park SJ, Nam M, Kang J, Kim K, Yeo JH, et al. A Variant of SLC1A5 Is a Mitochondrial Glutamine Transporter for Metabolic Reprogramming in Cancer Cells. *Cell Metab* 2020;31:267-83.e12.
14. Lu SC. Glutathione synthesis. *Biochim Biophys Acta* 2013;1830:3143-53.
15. Kennedy L, Sandhu JK, Harper ME, Cuperlovic-Culf M. Role of Glutathione

- in Cancer: From Mechanisms to Therapies. *Biomolecules* 2020;10.
16. Magaway C, Kim E, Jacinto E. Targeting mTOR and Metabolism in Cancer: Lessons and Innovations. *Cells* 2019;8.
 17. Tesfay L, Paul BT, Konstorum A, Deng Z, Cox AO, Lee J, et al. Stearoyl-CoA Desaturase 1 Protects Ovarian Cancer Cells from Ferroptotic Cell Death. *Cancer Res* 2019;79:5355-66.
 18. Li J, Cao F, Yin HL, Huang ZJ, Lin ZT, Mao N, et al. Ferroptosis: past, present and future. *Cell Death Dis* 2020;11:88.
 19. Xu FL, Wu XH, Chen C, Wang K, Huang LY, Xia J, et al. SLC27A5 promotes sorafenib-induced ferroptosis in hepatocellular carcinoma by downregulating glutathione reductase. *Cell Death Dis* 2023;14:22.
 20. Roh JL, Kim EH, Jang H, Shin D. Nrf2 inhibition reverses the resistance of cisplatin-resistant head and neck cancer cells to artesunate-induced ferroptosis. *Redox Biol* 2017;11:254-62.
 21. Conrad M, Kagan VE, Bayir H, Pagnussat GC, Head B, Traber MG, et al. Regulation of lipid peroxidation and ferroptosis in diverse species. *Genes Dev* 2018;32:602-19.
 22. Nakano Y, Tanno S, Koizumi K, Nishikawa T, Nakamura K, Minoguchi M, et al. Gemcitabine chemoresistance and molecular markers associated with gemcitabine transport and metabolism in human pancreatic cancer cells. *Br J Cancer* 2007;96:457-63.
 23. Davidson JD, Ma L, Flagella M, Geeganage S, Gelbert LM, Slapak CA. An increase in the expression of ribonucleotide reductase large subunit 1 is associated with gemcitabine resistance in non-small cell lung cancer cell lines. *Cancer Res* 2004;64:3761-6.
 24. Gao Y, Zhang Z, Li K, Gong L, Yang Q, Huang X, et al. Linc-DYNC2H1-4 promotes EMT and CSC phenotypes by acting as a sponge of miR-145 in pancreatic cancer cells. *Cell Death Dis* 2017;8:e2924.
 25. Funamizu N, Honjo M, Tamura K, Sakamoto K, Ogawa K, Takada Y. microRNAs Associated with Gemcitabine Resistance via EMT, TME, and Drug Metabolism in Pancreatic Cancer. *Cancers (Basel)* 2023;15.
 26. Sun Y, Liu Y, Ma X, Hu H. The Influence of Cell Cycle Regulation on Chemotherapy. *Int J Mol Sci* 2021;22.
 27. Infantino V, Santarsiero A, Convertini P, Todisco S, Iacobazzi V. Cancer Cell Metabolism in Hypoxia: Role of HIF-1 as Key Regulator and Therapeutic Target. *Int J Mol Sci* 2021;22.
 28. Wu S, Zhu C, Tang D, Dou QP, Shen J, Chen X. The role of ferroptosis in lung cancer. *Biomark Res* 2021;9:82.
 29. Xie Y, Hou W, Song X, Yu Y, Huang J, Sun X, et al. Ferroptosis: process and function. *Cell Death Differ* 2016;23:369-79.
 30. Sappington DR, Siegel ER, Hiatt G, Desai A, Penney RB, Jamshidi-Parsian A,

- et al. Glutamine drives glutathione synthesis and contributes to radiation sensitivity of A549 and H460 lung cancer cell lines. *Biochim Biophys Acta* 2016;1860:836-43.
31. Sun Y, Zheng Y, Wang C, Liu Y. Glutathione depletion induces ferroptosis, autophagy, and premature cell senescence in retinal pigment epithelial cells. *Cell Death Dis* 2018;9:753.
 32. Shimano H, Sato R. SREBP-regulated lipid metabolism: convergent physiology - divergent pathophysiology. *Nat Rev Endocrinol* 2017;13:710-30.
 33. Yi J, Zhu J, Wu J, Thompson CB, Jiang X. Oncogenic activation of PI3K-AKT-mTOR signaling suppresses ferroptosis via SREBP-mediated lipogenesis. *Proc Natl Acad Sci U S A* 2020;117:31189-97.
 34. Wattanawongdon W, Hahnvajanawong C, Namwat N, Kanchanawat S, Boonmars T, Jearanaikoon P, et al. Establishment and characterization of gemcitabine-resistant human cholangiocarcinoma cell lines with multidrug resistance and enhanced invasiveness. *Int J Oncol* 2015;47:398-410.
 35. Jia Y, Xie J. Promising molecular mechanisms responsible for gemcitabine resistance in cancer. *Genes Dis* 2015;2:299-306.
 36. Zilka O, Shah R, Li B, Friedmann Angeli JP, Griesser M, Conrad M, et al. On the Mechanism of Cytoprotection by Ferrostatin-1 and Liproxstatin-1 and the Role of Lipid Peroxidation in Ferroptotic Cell Death. *ACS Cent Sci* 2017;3:232-43.
 37. Martín-Saiz L, Guerrero-Mauvecin J, Martín-Sánchez D, Fresnedo O, Gómez MJ, Carrasco S, et al. Ferrostatin-1 modulates dysregulated kidney lipids in acute kidney injury. *J Pathol* 2022;257:285-99.
 38. Rawla P, Sunkara T, Gaduputi V. Epidemiology of Pancreatic Cancer: Global Trends, Etiology and Risk Factors. *World J Oncol* 2019;10:10-27.
 39. Grasso C, Jansen G, Giovannetti E. Drug resistance in pancreatic cancer: Impact of altered energy metabolism. *Crit Rev Oncol Hematol* 2017;114:139-52.
 40. Cha YJ, Kim ES, Koo JS. Amino Acid Transporters and Glutamine Metabolism in Breast Cancer. *Int J Mol Sci* 2018;19.
 41. Yang Q, Li K, Huang X, Zhao C, Mei Y, Li X, et al. lncRNA SLC7A11-AS1 Promotes Chemoresistance by Blocking SCF(β -TRCP)-Mediated Degradation of NRF2 in Pancreatic Cancer. *Mol Ther Nucleic Acids* 2020;19:974-85.
 42. Xue D, Zhou X, Qiu J. Emerging role of NRF2 in ROS-mediated tumor chemoresistance. *Biomedicine & Pharmacotherapy* 2020;131:110676.
 43. Porstmann T, Santos CR, Griffiths B, Cully M, Wu M, Leevers S, et al. SREBP activity is regulated by mTORC1 and contributes to Akt-dependent cell growth. *Cell Metab* 2008;8:224-36.

44. Chen X, Kang R, Tang D. Ferroptosis by Lipid Peroxidation: The Tip of the Iceberg? *Front Cell Dev Biol* 2021;9:646890.

ABSTRACT(IN KOREAN)

췌장암의 약물내성을 억제하는 새로운 치료제 유전자 발굴

< 지도교수 정재호 >

연세대학교 대학원 의과학과

김명진

췌장암은 초기 발견이 어려워 다른 암에 비해 5년 생존율이 낮아 예후가 좋지 않습니다. 췌장암의 대표적인 치료제인 췌시타빈은 약물저항성으로 인해 환자에게 좋지 않은 결과를 보이는 경우가 많습니다. 따라서 췌시타빈에 대한 내성을 극복하기 위해서는 새로운 target을 찾아야 합니다. 본 연구에서는 글루타민 수송체인 SLC38A5가 췌시타빈에 민감한 환자보다 췌시타빈 내성 환자에서 더 과발현된다는 사실을 발견했습니다. 또한, SLC38A5의 결실은 췌시타빈 내성 췌장암 세포의 증식 및 이동을 감소시켰습니다. SLC38A5의 억제자 RNA 염기서열 분석을 통해 폐롭토시스를 촉발한다는 사실도 발견했습니다. SLC38A5를 억제하면 미토콘드리아 기능 장애가 유발되고 글루타민 흡수 및 글루타치온 수준이 감소했으며 글루타치온 관련 유전자인 NRF2와 GPX4의 발현이 감소하였습니다. 글루타민 흡수 차단은 mTOR-SREBP1-SCD1 신호 전달 경로를 하향조절 했습니다.

따라서 SLC38A5의 억제는 지질 ROS 수준을 조절하는 두 가지 경로를 통해 폐롭토시스를 유발합니다. 또한 in vivo 실험을 통해 중앙 성장과 전이를 방해함으로써 SLC38A5의 억제가 췌시타빈 민감성을 회복시키는 것을 확인했습니다. 전체적으로, 본 연구는 SLC38A5가 췌장암 치료에서 췌시타빈 내성을 극복하기 위한 새로운 치료 표적이 될 수 있음을 입증했습니다.

핵심되는 말 : SLC38A5, 췌시타빈 내성, 췌장암, 지질 ROS, 폐롭토시스